Aerosol Gel Production Via Controlled Detonation of Liquid Precursors

by

Sarah Elizabeth Gilbertson

B.S., Kansas State University, 2006

A Thesis

submitted in partial fulfillment of the requirements for the degree

Master of Science

Department of Physics
College of Arts and Sciences

Kansas State University
Manhattan, Kansas
2008

Approved by:

Major Professor
Dr. Christopher M. Sorensen

Abstract

This work emphasizes advancements in Aerosol Gelation. We have attempted to expand the available materials used to synthesize Aerosol Gels by moving away from gas phase precursors toward liquid phase precursors and eventually reactants in the solid phase. The primary challenge was to efficiently administer the liquid fuels into the detonation chamber. After several attempts, it was concluded that the most efficient delivery technique was to heat the liquid fuel past the vapour point and evaporate it into the oxidizing gas for combustion. This method consistently yields soot with a density of 3.2 mg/cc approximately 10 minutes after the combustion. It was concluded that four criterion must be met to create an Aerosol Gel from a liquid:

1. The liquid must be as finely divided as possible
2. The energy of the spark must be large enough to cause a sustainable combustion
3. The fuel must have a Lower Explosive Limit above the necessary concentration to meet a volume fraction of 10^{-4}
4. The fuel must have a relatively low boiling point

Table of Contents

List of Figures

List of Tables

Acknowledgments

This work was funded by Targeted Excellence as a part of the Indoor Air Quality Control Research and Development grant. The work was carried out at Kansas State University in the Department of Physics in the labs and under the supervision of Dr. Chris Sorensen. I would like to thank Dr. Kenneth Klabunde for use of his BET, XRD, and UV Spectrometer instruments and I would also like to thank Dr. Daniel Boyle for TEM work. I would like to thank Russ Reynolds and Bryan Merritt for their impressive machining and James Hodgeson for his superior glass blowing skills. I would also like to thank Scott Chainey for his time for consultations on circuit designs and troubleshooting.
I would also like to thank Dr. Amit Chakrabarti and Dr. Bruce Law for agreeing to be on my committee and taking the time to read this work and assist me with any questions I have had.

Dedication

I would like to dedicate this publication to my husband who is an encouragement no matter what I do and to Dr. Sorensen who has become close enough to be considered family. Thanks for everything you have done to help me succeed.

Chapter 1

Introduction

1.1 Background On The Gelation Process

The gelation process is not a new phenomena. As early as 1931[4], researchers were creating novel, low density gels using various methods. One of the most well known methods of gelation is the sol-gel method. This process, as illustrated in Figure (1.1), involves mixing two liquid chemicals to form a precipitant. This precipitant forms a polymer network by a gradual change of liquid monomers into a polymeric sol, which subsequently gels. In most cases, this is then heated to remove any remaining liquid by evaporation and to pyrolyse the system.

The result is a rigid, low density material with a high specific surface area and porosity. In addition, the physical properties of the gel differ from those of other forms of the same material. One example is an aerogel made of SiO_2 in comparison with sand one might find on a beach. Because of these unique properties, there are a wide range of applications for such materials. So vast are these applications, in fact, that it would be inappropriate to attempt to list them all here. Therefore, those of particular interests and relevance to this project will be introduced only.

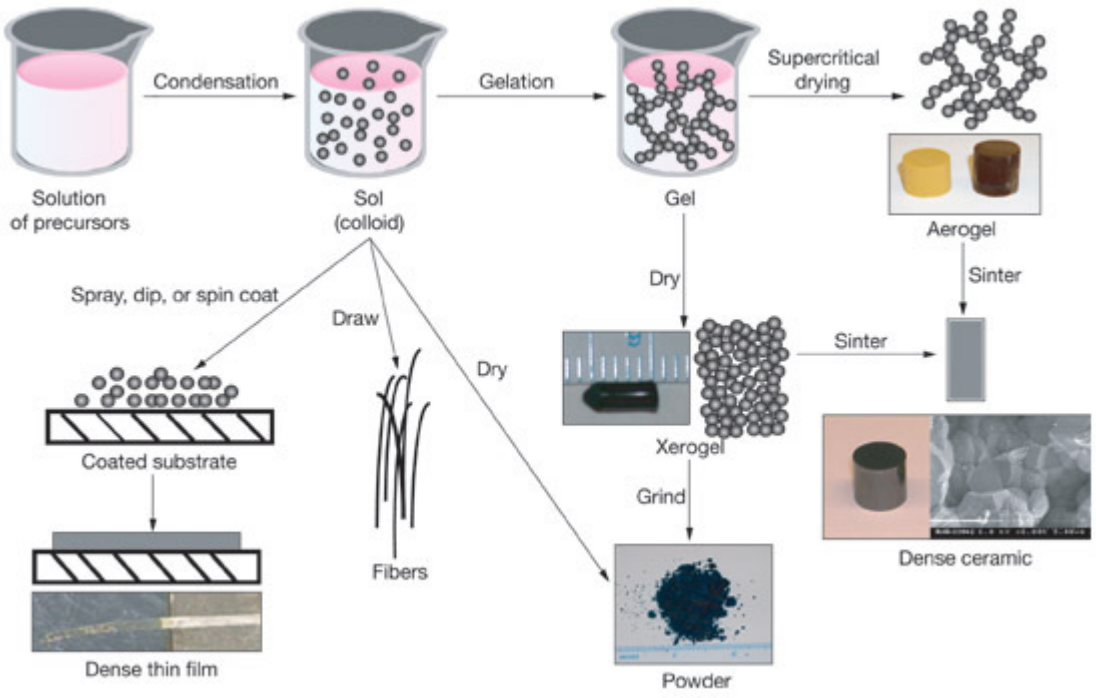

Figure 1.1: The Sol-gel method of gelation.[1]

A current area for application is the use of gels in creating ultra-thin coatings for either insulation purposes or for photocatalytic layers. By referring to Figure (1.1), it can be seen how the sol-gel process is modified to form different types of gels, each used for different applications. It is important, and I dare say the focus of this work, to note that the sol-gel process is not the only method by which a gel is made.

This work is about developments in the Aerosol Gelation process; a competitive process to the sol-gel method. In order to better understand the relationship between Aerosol Gels and the two main gels synthesized via the sol-gel process, each must be described in their own fashion.

1.2 Aerogels, Xerogels and Aerosol Gels

1.2.1 Aerogels

Aerogels are made beginning with a sol-gel process. The solvent is evaporated away by elevating the temperature and the pressure. In doing so, only the polymer network remains and the solvent is replaced by a gas; typically air, which constitutes the bulk of the solid. The gel must be critically dried in this fashion if it is to retain a low density and to prevent the network from collapsing. As a result of this procedure, the properties of the material are dramatically different than other forms. "Silica aerogels have been fabricated with bulk densities in the range of 0.003 [to] 0.35 g/cm^3, index of refractions from 1.0 [to] 1.05, thermal conductivities from 0.008 [to] 0.017 W/mK, and tensile strengths of 16 kPa or higher[5]." An image of a silica Aerogel can be seen in Figure (1.2)

Aerogels can be made from a variety of precursors, both metallic and non-metallic, so long as they are reactive with a hydrolysing agent. Metal alkoxides are generally used because they readily react with water to produce the polymer and an alcohol.

In spite of the unique properties these materials posses, the complexity of this critical drying process as well as the time scale to complete it (generally over 24 hours), makes the aerogel process unsuitable for large scale implementation. The process is also limited to precursors which react to form precipitants.

1.2.2 Xerogels

Xerogels, like aerogels, begin with a sol-gel process. The difference in the two process comes in how they are dried. After the sol gel reaction is complete, xerogels are allowed to dry under ambient pressure and temperature conditions. This causes a partial collapse of the polymer network resulting in a higher density aerogel. "[A]erogels are typically 90-99% air while xerogels are 60-90% air[5]."

Figure 1.2: An example of the thermal insulating properties of a silica aerogel[2]

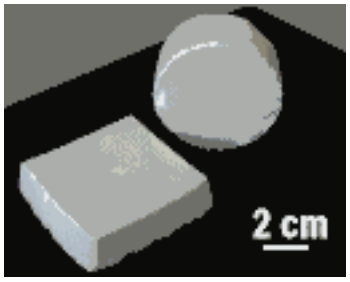

Figure 1.3: An example of a silica xerogel

1.2.3 Aerosol Gels

Aerosol gels are relatively new in comparison with the other two types offered here for comparison. Rather than beginning with a liquid phase sol-gel process to create the monomers and assemble them, the aerosol gels rely on a gas phase combustion process and the monomers self assemble into the polymeric chains by random walk and van der Waal's adhesion. Though constructed in a slightly different mechanism, the results are similar to gels synthesized via the sol gel method and there are only a few differences in the processes.

Figure 1.4: A picture of a silica Aerosol Gel which is approximately 10 cm long.

The density of the gels produced from this method falls within 2 to 8 mg/cc, making it the lowest density solid ever created and aiding to it's competitive stance with the aerogels and xerogels. Another difference is that there is no need for a critical drying stage in the aerosol gel process. This means that larger amounts of gel can be created in a shorter time frame, making it a more desirable process for commercial applications.

Therefore, it is useful to understand how the combustion process works and to more deeply understand the physics of the gelation process.

1.3 Chemistry of a Combustion Process

The process of combustion can be explained using molecular orbital theory. In order for a combustion to occur, a relatively high amount of energy is required to initiate the process. Combustions are self sustaining, so long as the oxidizer and the fuel are present in sufficient quantities. The reason that a high initial energy is required is largely due to the electronic configuration of the O_2 molecule.

O_2 has three bonded electron pairs and two unpaired electrons whose spins are aligned. These two electrons are responsible for the paramagnetic properties of O_2 and cause the molecule to have a non-zero net angular momentum. Most fuels, such as acetylene, consist of paired spins and have a zero net angular momentum. As such, a mixture of a hydrocarbon

and O_2 is stable under normal conditions and there is a very low probability of interaction between the fuel and the oxidizer

If energy is applied to the system, however, the O_2 molecule is forced into an excited singlet state, which is extremely reactive. The instability within spin-paired O_2 provides sufficient energy to rip a hydride radical from a neighbouring hydrocarbon. This process creates the first of many intermediates called the super oxide radical (HOO or hydroperoxide). Being equally reactive, super oxide extracts yet another hydride radical, which forms hydrogen peroxide, and then splits to create hydroxide radicals.

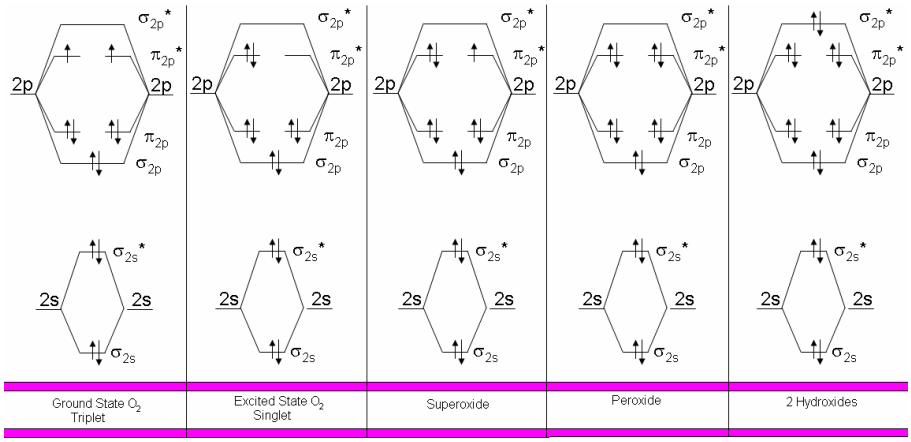

Figure 1.5: The change in MO configuration for the oxygen as the combustion progresses.

1.3.1 Dehydrogenating Hydrocarbons

Throughout the combustion, the oxidizing agent is constantly pulling hydrogen atoms away from the hydrocarbons, causing them to constantly reconfigure to achieve the lowest possible energy state. The fuel is broken down into methyl groups which combine to form hydrocarbon chains. As more hydrogen atoms are removed, the chains curl into aromatic rings. These rings begin to combine into polyaromatics forming graphitic spheriles that coalesce during collisions. Once the dehydrogenation process is complete, the spheres are primarily hard, carbon balls on the order of 10 to 30 nm.

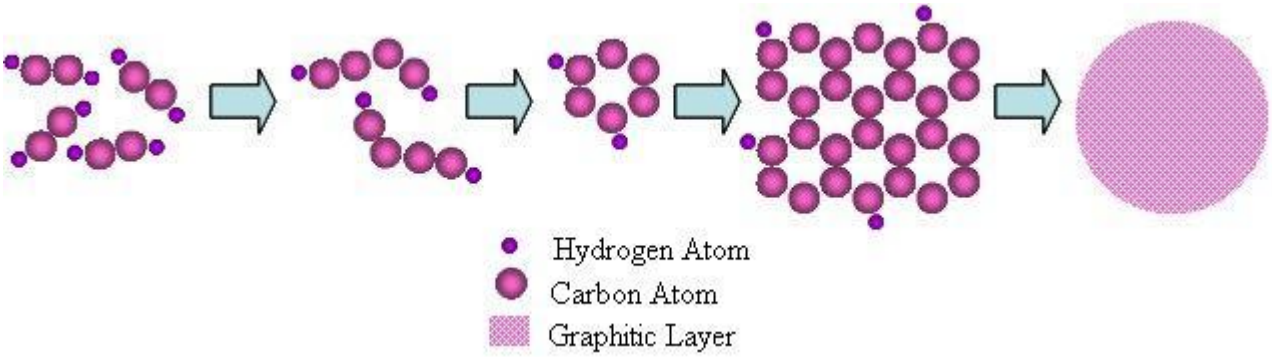

Figure 1.6: The evolution from molecular hydrocarbons to nanoscale graphitic spheres via dehydrogenation

The time scale of this reaction can be from 10^{-10}s to slightly less than 1s[6].

Chapter 2

Theoretical Considerations

2.1 Volume Fraction and Fractal Aggregates

In order to thoroughly understand the process by which a system is constructed, we must first understand the manner in which particles assemble. This is best understood from a knowledge of volume fraction as well as fractal aggregation.

2.1.1 Volume Fraction

The volume fraction is the fraction of space which is occupied by solid matter with in a substance. The reason that gels are low density materials is because there is a comparatively low amount of occupied space relative to nearly all other solids.

To understand this better, let us consider a regular, crystalline structure. Figure (2.1) shows a body centered cubic crystal, drawn as a unit cell. At each corner of the unit cell are one eighth of a sphere with an entire sphere in the center. Since there are eight corners all together, there are a total of 2 spheres contained within one unit cell. Each of these spheres has a volume of $\frac{4}{3}\pi a^3$ which means that the total volume of occupied space is

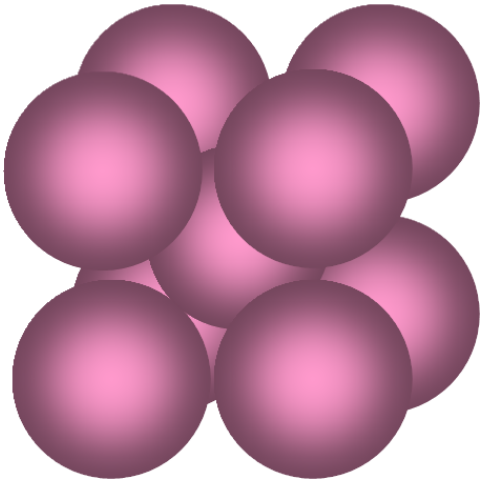

Figure 2.1: A Body Centered Cubic Crystalline Structure.

$$V_{occupied} = \frac{8}{3}\pi a^3 \tag{2.1}$$

This is not the total space of the cell, however. The volume of the cell is simply the cell length cubed. We can easily related this cell length to the radius of the sphere by noting that the center diagonal is $4a$ in length. After a small amount of geometry we arrive at

$$l = \frac{4\sqrt{3}}{3}a$$

Which yields a cell volume of

$$V_{cell} = \left(\frac{16}{3}\right)^{\frac{3}{2}} a^3 \tag{2.2}$$

Therefore, the fraction of available space which is occupied, or the volume fraction, is just the ratio of used space to available space.

$$f_v = \frac{V_{occupied}}{V_{cell}} \approx 0.68 \tag{2.3}$$

This tells us that in a crystal with a body centered cubic structure, 32% of the substance is empty space. As was previously mentioned, gels are nearly 95% empty space and have a volume fraction of 10^{-4} rather than $\approx 10^{-1}$. This is largely attributed to the fractal nature of the gel, which is the next area of quantification.

2.1.2 Fractal Aggregate

To understand what a fractal is, one first must re-examine the idea of dimension. There are two ways to consider a dimension. The most common is the concept of degrees of freedom. For example, a line has one degree of freedom. We can either move left or right along the line, depending on how we define our coordinates. A plane has two degrees of freedom. Now we can move left or right or up or down.

Mathematically we can expand upon this idea with the notion of vectors. A line only has 1 linearly independent vector which can describe it while a plane has 2 and a cube has 3, etc. All vectors within the space can be reduced into components or parts of these vectors.

Fractal dimensions are best understood by considering a scaling argument rather than a degrees of freedom approach. A tangible example of this is the scaling of mass in comparison to the scaling of surface area. If an object is made twice as big and kept in proportion, it must increase in width, height and depth. So, its mass, related to it's volume by density, increases by a factor of

$$m = 2 \times 2 \times 2 = 2^3 = 8$$

Volume scales three ways while surface area scales by a factor of two. The surface area of the object therefore increases by

$$A = 2 \times 2 = 2^2 = 4$$

Thus, by doubling the linear size of an object, it's mass is increased eight times while it's

surface area only increases by four times. While there are interesting biological observations which can be made here relating to the proportions of limbs and metabolisms in large versus small creatures, as physicists we are more interested in the scaling factors. Notice, that mass scales to the third power while area scales as the square.

$$m \propto l^3$$

$$A \propto l^2$$

Where l is a linear length scale.

Another way we could look at this is to say that both mass and area scale to the dimension of the shape, 3-dimensional for mass and 2-dimensional for area. With this concept understood, we can re-write the relationship of mass to dimensionality, d, as

$$m \propto l^d$$

or

$$\ln(m) \propto d \ln(l)$$

We can generalize this relationship to any system with or without an integer scaling dimension with the following relation:

$$\ln(m) \propto D \ln(l) \tag{2.4}$$

Graphically, if we were to plot mass versus length using logarithmic scales, we would get a straight line, whose slope was equal to the dimension of the object. A plot of mass as a function of distance ($m(r)$) of a fractal plotted versus the distance yields a slope of 1.8, not 1 or 2.

It should now be clear that a fractal is a scale invariant solid with a non-integer scaling dimension.

2.2 Conditions for Gelation

Gelation is the process by which particles aggregate into clusters which subsequently aggregate into a large singular network that spans the space of the container.

In work done by Dhaubhadel, Gerving, Chakrabarti, and Sorensen in 2006, it was asserted that "any system of particles undergoing aggregation can form a gel if the combining particles do not coalesce and if the time to reach the gel point is shorter than other time scales that can deter gel formation.[7]"

To compute the gel time, consider a system of N_{system}, non-coalescing particles in a space with a volume V_{system}. As these particles aggregate, they will form cluster networks. A single cluster will have N_o number of particles and will occupy a volume of V_o. This is illustrated in Figure (2.2).

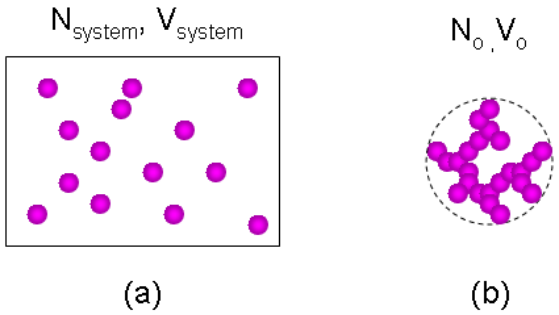

Figure 2.2: The number of particles and volume of (a) a system of particles, and (b) a cluster

The number densities of each case is given by the number of particles divided by the

volume.

$$n_{system} = \frac{N_{system}}{V_{system}} \tag{2.5}$$

$$n_{cluster} = \frac{N_o}{V_o} \tag{2.6}$$

Because mass is conserved, the total number of particles in the system should be equal to the number of particles in a single cluster times the number of clusters.

$$N_{system} = N_{\text{total clusters}} N_o \tag{2.7}$$

Similarly, the total number of clusters multiplied by the volume of each cluster should give the total cluster volume.

$$V_{\text{total clusters}} = N_{\text{total clusters}} V_o \tag{2.8}$$

Combining Equations (2.5), (2.7), and (2.8) yields the following relationship

$$n_{system} V_{system} = n_c V_{\text{total clusters}}$$

or,

$$n_{system} = n_c \frac{V_{\text{total clusters}}}{V_{system}} \tag{2.9}$$

A system is said to have gelled when the clusters span the space of the containter. Under that condition, $V_{system} \approx V_{\text{total clusters}}$ and therefore:

$$n_{system} = n_{cluster} \tag{2.10}$$

This is fine for a macroscopic system where both N and V are measureable, but in a

nanosystem, N is easier to determine in another fashion. If we start with a single monomer of radius a allow it to aggregate in the Sorensen-Oh method described in the previous chapter, we start to notice that a large cluster can be seen as an aggregation of smaller clusters. We can define the radius of these smaller clusters as R as seen in Figure (2.3a) and Figure (2.3b), below.

Figure 2.3: Radius of gyration of fractal aggregates

(a) A monomer of radius a in an aggregate with a radius R

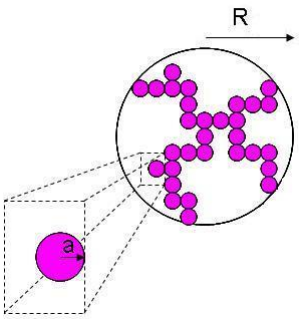

(b) Several aggregates have clustered to form a larger network

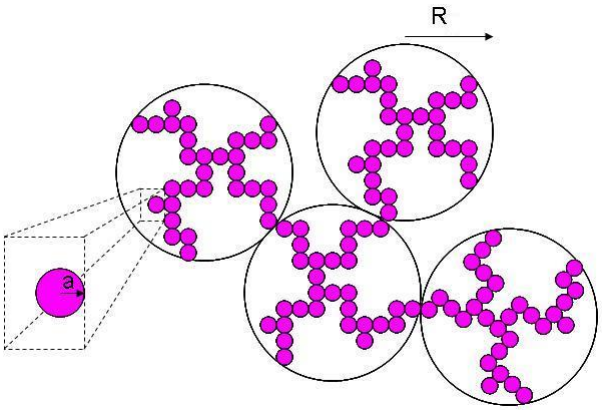

For a fractal aggregate, the size scales as the fractal dimension, D rather than the spatial dimension, d [1]. We can express this as

$$N_o \approx \left(\frac{R}{a}\right)^D \tag{2.11}$$

We can now substitute Equation (2.11) into Equation (2.6), and we see

$$n_{cluster} = \frac{3N}{4\pi R^3} = \frac{3R^{D-3}}{4\pi a^D} \tag{2.12}$$

[1] D is always less than d

The volume fraction of the system can be expressed as

$$f_v \approx n_{system} a^3 \tag{2.13}$$

Now, by combining Equations (2.10), (2.12), and (2.13) we can arrive at the approximate size of the clusters at the gel point.

$$R_{gel} = a \left(\frac{3 f_v}{4\pi} \right)^{\frac{1}{D-3}} \tag{2.14}$$

In this sort of experiment, time scales are key. A gel will not form if it takes longer to aggregate than it takes to settle. We can use Equation (2.14) to determine how long it will take to gel under ideal conditions. Cluster growth is described by the Smoluchowski Equation, which is given in Equation (2.15).

$$\frac{dn_{cluster}}{dt} = -K n_{cluster}^2 \tag{2.15}$$

Where K is a constant dependent on the thermal energy and viscosity of the background gas.

It is seen from the solution of Equation (2.15) that the number density changes as a function of time. When the system has finally gelled, the number density of the system is

$$n_gel = n_{system} \left(t = t_{gel} \right) \tag{2.16}$$

It can therefore be stated that:

$$n_{gel} = N_o \left(t \right) n_{cluster} \left(t \right) \tag{2.17}$$

where the limiting case results in Equation (2.10)

Combining Equation (2.11) with Equation (2.14) gives

$$n_{cluster} = \frac{n_{gel}}{f_v^{\frac{D}{(D-3)}}} \tag{2.18}$$

Finally, combining Equation(2.18) with Equation (2.13) and substituting the result into Equation (2.19) we arrive at the gel time.

$$t_{gel} = \frac{a^3 f^{\frac{-3}{(3-D)}}}{K} \tag{2.19}$$

When we input the fractal dimension for a DLCA aggregate, $D = 1.8$, Equation 2.19) becomes

$$t_{gel} \approx \frac{a^3 f_v^{-2.5}}{K} \tag{2.20}$$

Figure (2.4) shows the gel time as a function of volume fraction for three different radii of monomeric particles. An analysis of this graph shows that the two most important conditions for gelation are a volume fraction of 10^{-4} or more and a monomer radius on the order of tens of nanometers or less, if we are to achieve convenient aggregation times.

"The conditions for rapid gel formation ... can be obtained with rapid, gas phase reactions... Rapid reactions from the gas to solid phase will drive the system deep into a supersaturated regime" and the uniform nucleation of nano particles will occur[7]. Work carried out by Dhaubhadel et al. focussed on using gas phased precursors in their reactions. Since this work focusses on liquid phase precursors, it is important to understand the physics of changing phases to the gas regime for the most effect gelation. First, however, we must discuss what is meant by Volume Fraction and Fractal Aggregation.

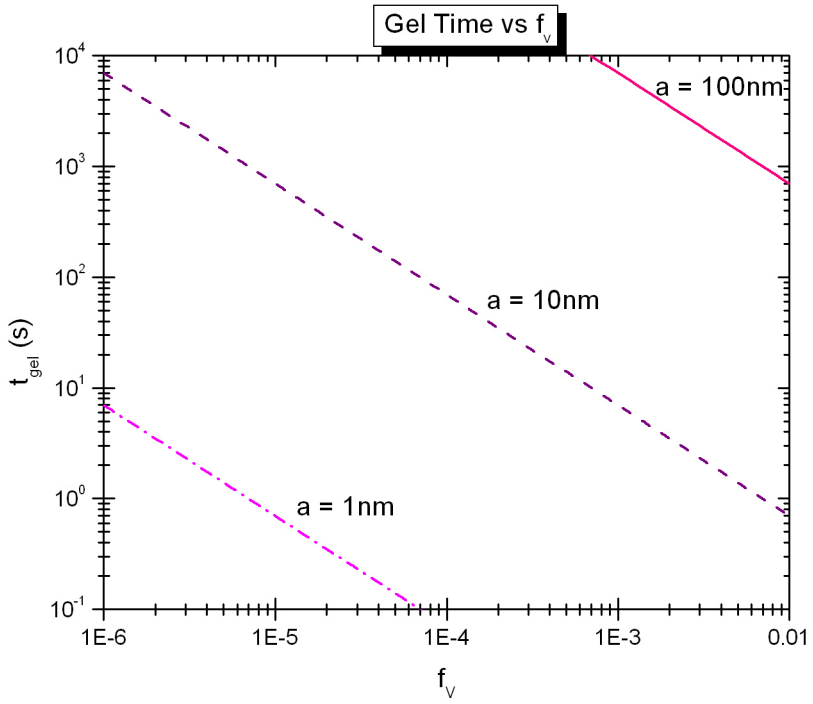

Figure 2.4: The time for gelation as a function of volume fraction for various radii of particles.

2.3 Pressure Calculations

2.3.1 Vapor Pressure Curves

Evaporation occurs when the pressure above the liquid exceeds the vapour pressure of the liquid at a given temperature. Evaporation will continue until the gas above the liquid is saturated. Because the thermal kinetic energy of gasses increase with temperature, the air above a liquid can hold more vapour as the temperature increases. The vapour pressure of several different liquids are shown in the graph in Figure (2.5).

Vapour pressure is calculated using the Clausius-Clapyron equation and the values of enthalpy and entropy specific to the liquid.

$$\ln p = -\frac{\Delta H_{vap}}{RT} + \frac{\Delta S_{vap}}{R} \tag{2.21}$$

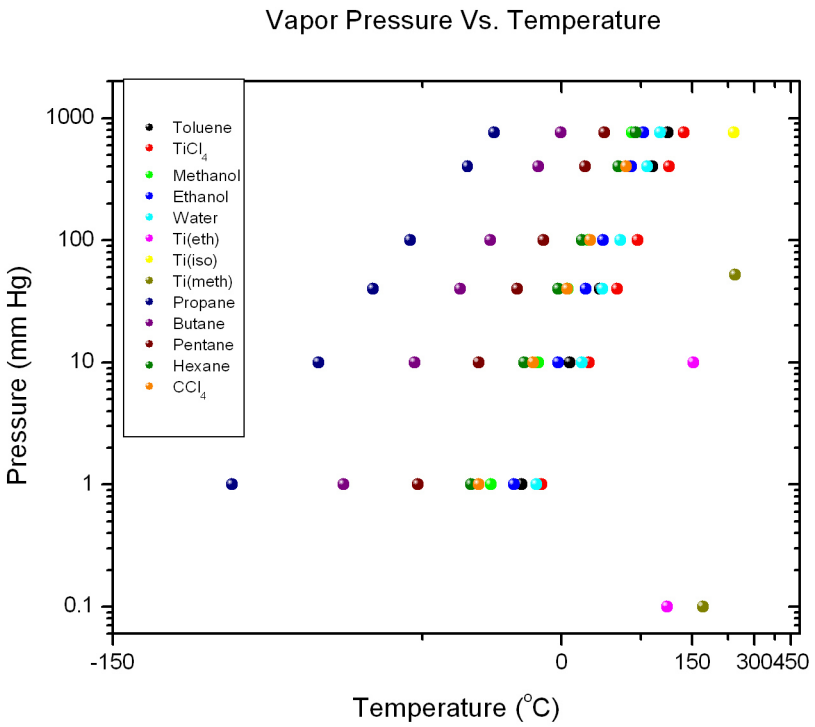

Figure 2.5: The Vapour Pressure as a Function of Temperature for a large variety of liquid fuel sources and other liquids.

2.3.2 Combustion Pressure Calculations

Since the Aerosol gels are made via a combustion method, safety is an important consideration. This part will pertain to calculations of the explosion pressure.

The energy released during a combustion can be determined from the following relation:

$$\Delta p = \frac{1}{V}\left[\sum_{products} m_i \Delta H_i - \sum_{reactants} m_i \Delta H_i - \Delta T \sum_{products} m_i C_{V,i} - p_o V \left(1 - \frac{\sum_{products} m_i}{\sum_{reactants} m_i}\right)\right] \tag{2.22}$$

Where m_i is the actual number of moles of the species, ΔH_i is the heat of formation of the species, and $C_{V,i}$ is the specific heat at constant volume of the species.

For acetylene this pressure change was approximately 57 atm, which compares with calculations done by Dhaubhadel[2]. The acetylene combustion is indicative of the pressure waves generated by most gas phase combustion under similar conditions.

The results of a complete combustion of styrene, however, are nearly 3 times those of Acetylene. This makes it unsafe to use any sort of quartz or glass windows in the detonation chamber. The other ports and attachments still fall within the safe operating range for these types of reactions.

[2]Personal Communication

Chapter 3

Experimental Methods

3.1 Introduction

The following chapter is intended to describe the different experimental approaches taken in attempting to synthesize Aerosol Gels from a liquid precursor. It is well known that liquid fuels burn from the bulk form (by bulk I mean a condensed form of the material, in this case liquid, on the order of a few mL to several gallons or more). It is also commonly understood that dividing this matter into a finer form yields a more energetic burn to the point of combustion. This is a principle upon which a fuel injector engine is designed.

Therefore, my primary goal was to develop a way of dividing the liquid into small droplets and deliver these droplets into the test chamber for detonation. For liquid droplets, the best forms for this are a vapour or an aerosol. What follows are descriptions of attempts at generating appropriate vapours and aerosols and the results of these efforts.

3.2 Approaches of Nebulization

3.2.1 Air Blast Nebulizer

The basic set up involved pumping air or O_2 into the Air Blast Nebulizer, which then carried the fuel into a 17 L test chamber for detonation.

Nebulizer Description

An Air Blast Nebulizer works largely on the Bernoulli effect by creating a low pressure area above a liquid reservoir and forcing the resulting aerosol around a series of right angles. This has two effects: first, the velocity of the gas jet is sufficient to break the surface tension of the liquid and create droplets. These droplets are usually polydispersed in terms of size. The second effect is to minimize the variation in droplet size and produce an aerosol that is as monodispersed as possible. This is accomplished by forcing the aerosol around right angles. The larger droplets are unable to complete the turns and impact along the walls, leaving only the smaller droplets in the flow.

A diagram of this nebulizer can be seen in Figure (3.1). The mixing of the carrier gas with the aerosol was appealing to us, which is one reason why this method was used. Another reason was convenience and what was then thought to be a small droplet size production.

Droplet Characterization

The droplet size was determined through a light scattering experiment carried out on a similar model nebulizer with an approximately equal nozzle diameter. This was found to be between 15μm and 18μm[8]. The droplet size of our set up was found to be approximately 20μm. This was found by spraying the mist into a closed chamber and measuring the settling time. Although this method has the potential for large amounts of error, it compares with measurements made by other researchers and is therefore our accepted value.

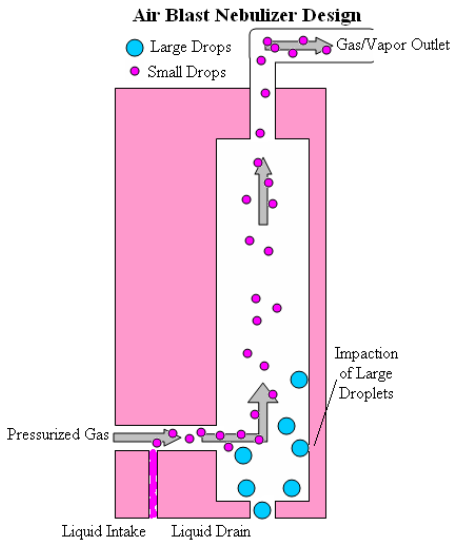

Figure 3.1: A diagram of the air blast nebulizer.

Syringe Pump Fed Liquid

It was quickly observed that there was insufficient liquid in the vapor, so we decided to attempt to increase the amount of liquid in the aerosol by pumping fluid into the atomizer rather than allowing it to draw it's own. Any droplets which were impacted, were collected again and subtracted from the original volume. In this way we were able to know the exact amount of liquid in the aerosol and it was hoped that we would gain more control of the volume fraction.

3.2.2 The Ultrasonic Nebulizer

The second approach was to use an ultrasonic nebulizer to generate and aerosol and fill the 17L chamber. The aerosol was transported to the 17L chamber using a gentle stream of air or O_2 , or a mixture of C_2H_2 and O_2 .

Nebulizer Description

The ultrasonic nebulizer uses an ultrasonic generator to drive a piezoelectric crystal at a fixed frequency. Chips can be purchased to operate between 200 kHz and 10 MHz. The surface of the liquid will break down when the longitudinal wave propagates from the crystal to the liquid-air interface. The wavelength of this wave is expressed in Equation (3.1).

$$\lambda = \left(\frac{8\pi\sigma}{\rho f^2}\right)^{\frac{1}{3}} \tag{3.1}$$

where λ is the wavelength, σ and ρ are the surface tension and density of the liquid, respectively, and f is the frequency of the piezoelectric device. The droplet diameter is given by Lang's constant times the wavelength. At MHz frequencies, the value of this constant is known to be 0.34. Therefore the average droplet size, D, can be determined from Equation (3.2)[9].

$$D = 0.34\left(\frac{8\pi\sigma}{\rho f^2}\right)^{\frac{1}{3}} \tag{3.2}$$

Design Distinction

There were two designs for the ultrasonic nebulizer. The first design had the PZT in a container where the oxidizer flowed over the vapour cloud and carried it into the 17 L chamber. The second design was a glass tube where the oxidizer was used to create a high pressure area over the vapour, pushing it into a straw-like tube and into a 100 mL chamber. Another difference between the two designs was the piezoelectric crystals. The PZTs used in the first design had an unknown resonant frequency and so appropriate driver circuitry could not be found. Those used in the second design were taken from a KAZ ultrasonic humidifier, available on-line for $19.98. The chip and circuitry were removed from the commercial device and fitted to the apparatus. Figure (3.2) shows the set up of the second

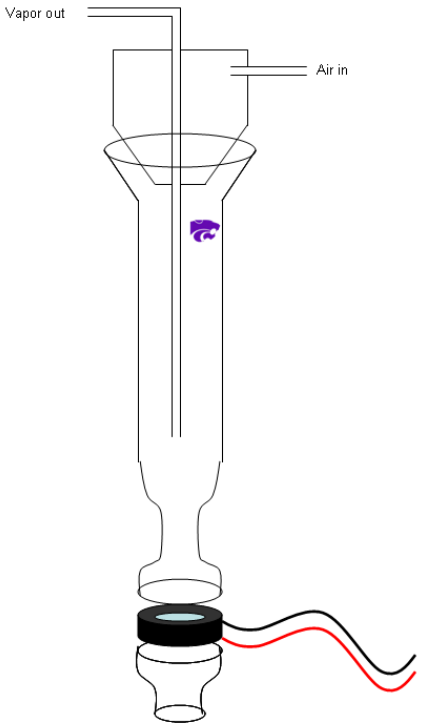

Figure 3.2: An example of the ultrasonic nebulizer. A side port was eventually added for working with moisture sensitive fuels.

design.

Droplet Characterization

The piezoelectric crystals which were available to me provided a frequency of 2.4 MHz. Using Equation (3.2) we see that the average droplet size is approximately 5.3 μm for styrene and 6.8 μm for water. I used light scattering to verify the droplet size and found them to be approximately 6 μm in diameter, which falls within the predicted range.

3.2.3 Fuel Injection Method

Description of Method

Fuel was loaded into a stainless steel reservoir that could withstand high pressures. The reservoir was then taken to 55 psi and a car fuel injector was activated, spraying the pres-

surized fuel into the 17 L chamber. The basics of how the liquid is made into droplets is similar to the air blast nebulizer, but this method allows for complete control of the volume of fuel being added to the system.

In order to understand how the droplets are generated, we must first consider the basic design of the fuel injector, as seen in the diagram in Figure (3.3). When a current is passed through the injector electromagnetic coil, the valve opens and the fuel pressure forces the fluid through the spray tip and out of the diffuser nozzle, atomising it as it does so. When current is removed, the combination of a spring and fuel back-pressure cause the needle valve to close. This on-off cycle time is known as the pulse width and varying the pulse width determines how much fuel can flow through the injectors.

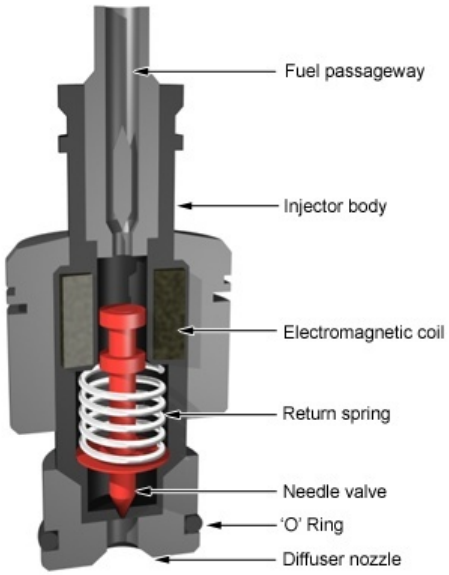

Figure 3.3: A schematic of the workings of a fuel injector[3]

Using a needed volume fraction of 10^{-4} I was able to determine the total amount of aerosolized fuel that would be needed. I adjusted the pulse width in two different ways to accomplish this. First, I established a series of short pulses and secondly, I applied one continuous pulse.

Droplet Characterization

The particular model of fuel injector used in this experiment was for a 1986 Buick Skylark and data from the manufacturer indicated that the average droplet size was on the order of 50 μm to 100 μm. Experimental observation qualitatively verified this information.

A summary of Nebulization techniques can be seen in Table (3.1) below.

Table 3.1: A list of the Nebulization Methods used and the average droplet size, $\bar{d}$, and maximum volume fraction, f_V, produced.

Technique	$\bar{d}(\mu m)$	f_V
Air Blast Nebulizer	15 - 18	10^{-5}
Ultra Sonic Nebulizer	5.3 - 6.8	10^{-4}
Fuel Injector	50 - 100	10^{-3}
Evaporation	≤ 1	10^{-4}

3.3 Results of Nebulization Methods

3.3.1 Air Blast Nebulizer

This method of introducing the liquid into the test chamber did not yield any soot after a combustion.

Main Restrictions

After we began experimentation with the Air Blast Nebulizer, we determined the following draw backs:

1. The nebulizer is only capable of aerosolizing a small volume of liquid. This generates a volume fraction of 10^{-5} in the very best scenario, which does not meet the criterion for gelation. The syringe pump method was unable to compensate for this set back, as can be seen in the graphs in Figure (3.4).

2. Only liquids with a small range of viscosities were appropriate for this method. This method did not work for liquids with viscosities appreciably higher than water (1-methyl naphthalene, for example). This puts an unreasonable limit on which materials are available for combustion under this method, making it undesirable.

3. Droplet size could not be controlled and was larger than desired. This factor was initially unknown to us. Larger droplets are undesirable because of the increased settling/coalescence time as well as an augmented tendency to pyrolyse rather than combust.

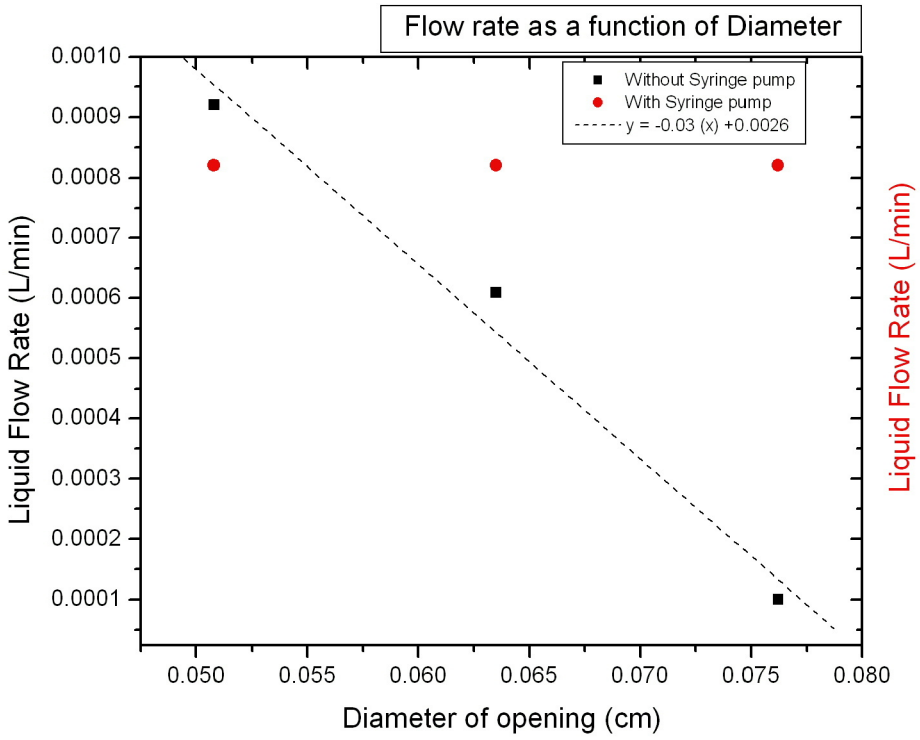

Figure 3.4: A graph of the liquid flow rate through an Air Blast Nebulizer with and without the aid of a syringe pump as a function of the diameter of the nozzle.

3.3.2 Fuel Injection Method

Although this method did combust, it did not yield desirable soot. One observation of this process was that it appeared we were spraying a garden hose into a bucket. As might be expected, the relatively large particle size is to blame, however, if we had not attempted this method, we would not have realized a very important parameter to the experiment.

Pyrolysis Versus Combustion of Droplets

To explain this method, first let us return to combustions of the gas phase. In this scenario, the fuel molecules do not shield one another from the oxidizer and a complete combustion is permitted. As the fuel becomes larger in bulk, only those molecules on the surface are free to interact with the oxidizer. This makes a difference between the *actual* and *interaction* volumes. A diagram of this can be seen in Figure (3.5).

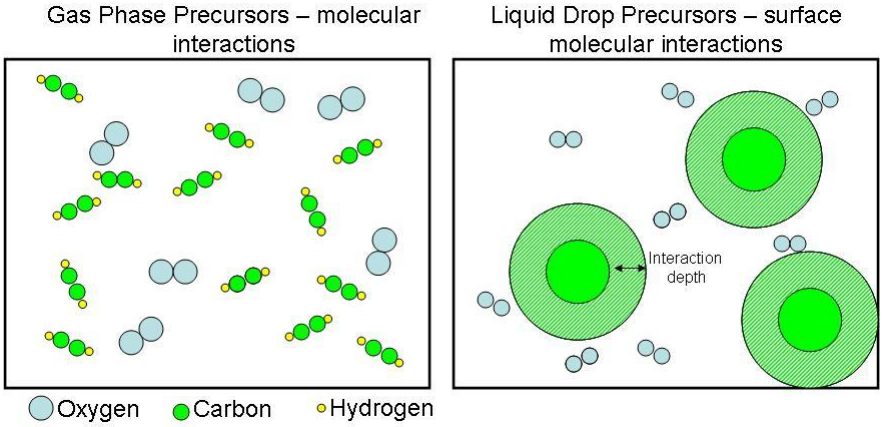

Figure 3.5: The difference in gas phase and liquid phase combustion reactions

(Find Source) One source indicates that depending on the material the interaction depth of a given material is between 10 $\mathring{A}$ and 100 $\mathring{A}$. This means that in order to utilize as much of the fuel as possible, the droplet size must be minimized. Essentially, the liquid must be brought as close to gas phase as possible before the combustion in order to optimize the resulting products.

If the droplets are too big, as were the case in this method, they will simply burn and harden as the liquid core evaporates away. This leaves shells of almost a micron in diameter, as seen in Figure (3.6).

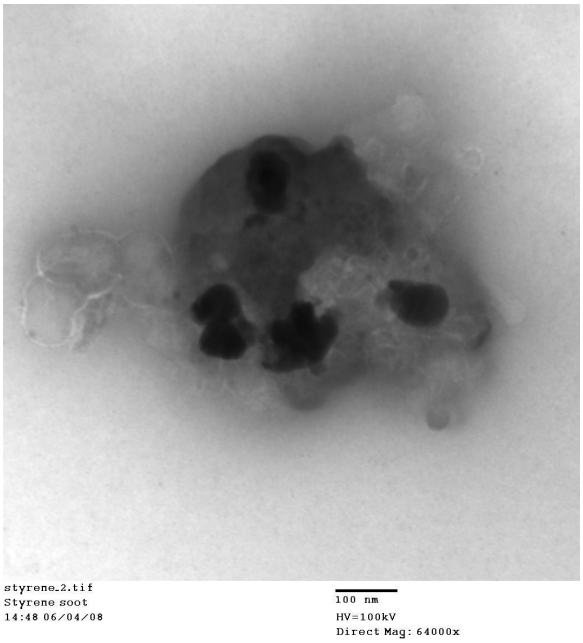

Figure 3.6: A TEM of a pyrolysed styrene droplet.

3.3.3 The Ultrasonic Nebulizer

Using the ultrasonic nebulizer, we were able to consistantly create a fine powder of soot. On occasion more quantities were also produced. Although it appears that the droplet size was still slightly too large, it was not the limiting factor. A measurement of volume fraction indicates slightly less than 10^{-4}. It is possible that the droplet size then played a stronger role in diminishing available fuel for reaction.

This form of nebulization is just at the limit of what is necessary to produce a light, fluffy gel.

Table 3.2: A list of the liquids used and their physical properties

Liquid	*Surface Tension* (N/m)	*Density* (kg/m^3)	*Viscosity* (N/m^2)	*Boiling Point* (^oC)	*Nebulize Easily?*
Water	0.072	997	1.0002	100	yes
Toluene	0.041	862	0.59	110.6	yes
Styrene	0.032	903	0.762	145	yes
$TiCl_4$	0.034	1333	0.826	136.4	yes
Titanium Ethoxide	0.023	99.9	125	122	no
Octane	0.021	700	0.542	126	yes
Ethanol	0.022	789	1.2	78.4	no
Butanol	0.025	810	3	117.73	no
Glycerol	0.064	1261	1069	290	no
Propanol	0.024	804	2.8	97	no
Pentane	0.015	626	0.36	36.1	yes

3.4 Fuel Selection, Handling, and Treatment

There are a lot of chemicals which could be suitable as a source of fuel. Before any experimentation could begin, I narrowed down a list of chemicals I would be working with. All chemicals were handled using proper protection and in most cases the fuel was handled under a fume hood. In the cases of some "less friendly" chemicals, chem aprons and respirators were also worn.

Table (??) enumerates the chemicals used and also lists various properties.

3.4.1 Selection of Hydrocarbons

In that the most successful method of nebulization was the ultrasonic nebulizer, it's parameters dictated the choices of fuels. One of the most sensitive parameters was the viscosity of the liquid chosen. As can be seen in Figure (3.7), if the viscosity is even slightly more than that of water, the liquid will not be broken down by the ultrasonic waves. Rather, it will splash against the sides of the container.

Another important consideration was sooting tendencies. Detailed calculations can be

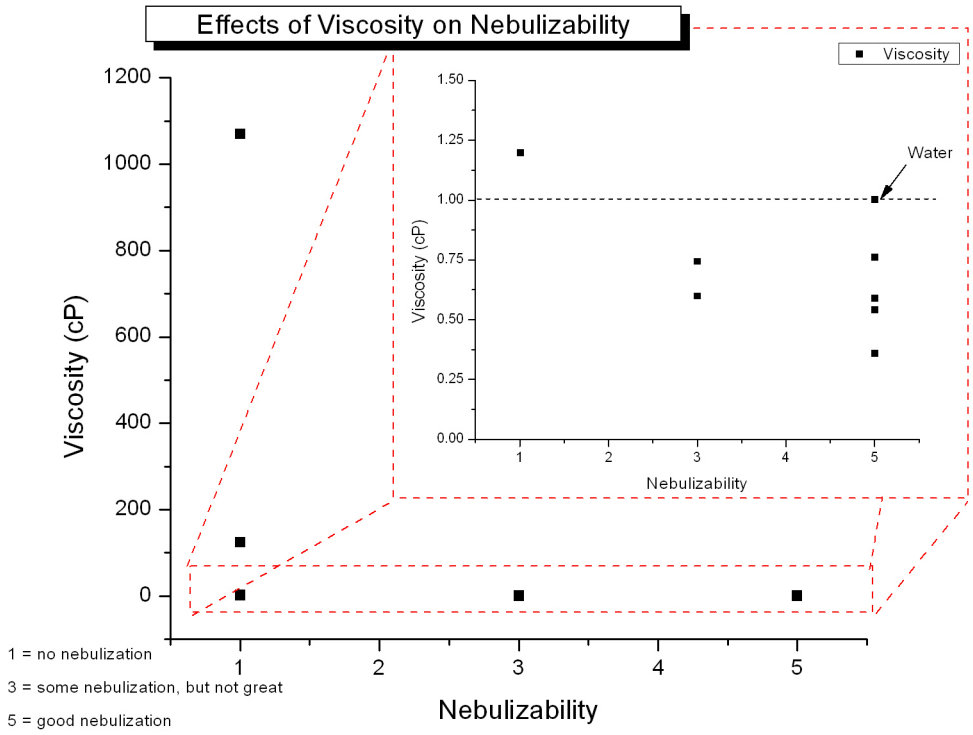

Figure 3.7: The effects of viscosity on the ease of nebulizability

made to determine the sooting tendency of a hydrocarbon under ideal conditions, but these calculations can be easily reduced to the ratio or carbon atoms to hydrogens. Benzene has a C to H ratio of 1, but it does not meet the requirements for a safe chemical to work with. So, two similar chemicals, toluene and styrene, were used in it's place.

3.4.2 Selection and Handling of Precursors to Photocatalytic Materials

A secondary goal of this project was to produce a novel photocatalytic material. Chemists already create gels made of TiO_2 which is photocatalytic in the UV spectrum. A focus of study is to attempt to shift the band gap in order to allow for photoactivity in the visible spectrum, thus making it useful for a variety of indoor applications.

Chemists mainly use Titanium isopropoxide or Titanium ethoxide, but neither of these chemicals were volatile enough under ambient conditions to be practicles in this experiment. Titanium tetrachloride met not only the volatility requirements, but the viscocity requirements as well.

3.5 Detonation Chamber Design and Considerations

Careful planning and safety considerations were made in the design of the detonation chamber. Several chambers were available for use in this experiment. These were designed by Dhaubhadel and Gerving and have a few notable features which are worthy of mention.

The Aluminum chamber built by Dhaubhadel was approximately 17L in volume and had 1 1/2 inch walls. It had optical ports for light scattering experiments and was originally intended for combustions of the gas phase. This chamber, massing approximately 90 kg, was difficult for me (massing 55 kg) to move and so a chassis was built with wheels and a pivot point to facilitate experimentation and transportation. The chamber was originally named Fat Man, but after the addition of this chassis, it more resembled the science fiction character R2D2, and was thus re-named accordingly.

Chapter 4

Analysis Techniques

There are numerous ways to characterize the Aerosol Gel and not all of them are familiar to physicists. This chapter will briefly describe the different techniques used to better understand our soot.

4.1 BET

BET is a technique for measuring the physical adsorption of gas molecules on a solid surface, which gives an indication of a material's specific surface area. Unlike most processes used in physics (such as TEM, for example), the acronym does not abbreviate the process, but rather stands for the initials of the three co-discoverers, Brunauer, Emmett and Teller.

BET works on three assumptions:

1. gas molecules physically adsorb on a solid in an unlimited number of layers
2. there is no interaction between each adsorption layer
3. Langmuir theory can be applied to each layer

The Langmuir adsorption equation relates the adsorption of molecules on a solid surface

to gas pressure or concentration of a medium above the solid surface at a fixed temperature. The resulting BET equation is given by[10]:

$$\frac{1}{v\left[(P/P_o)-1\right]} = \frac{c-1}{v_m c}\left(\frac{P}{P_o}\right) + \frac{1}{v_m c} \tag{4.1}$$

where P and P_o are the equilibrium and saturation pressures of the adsorbates at the temperature of adsorption, v is the adsorbed gas quantity, and v_m is the monolayer adsorbed gas quantity. c is the BET constant, which is expressed by

$$c = \exp\left(\frac{E_1 - E_L}{RT}\right) \tag{4.2}$$

where E_1 is the heat of adsorption for the first layer, and E_L is that for the second and higher layers and is equal to the heat of liquefaction.

Because surface area is related to particle size, this test is an important characterization and gives us an important basis for comparing our samples to other types of gels.

********** This Section is not Finished**********

I will connect this discussion with how this is a measurement of surface area.

4.2 BJH

While the BET technique uses a gas to measure the specific surface area of a porous substance, the BJH (also named for the discoverers rather than the process itself) uses a gas, usually nitrogen at 77K, to determine the size and general number of pores in the material. This is determined by a measurement of mass before and after adsorption and then a comparison of desorption at different pressures. This results in a hysteresis curve whose qualities indicate information of pore size.

First the sample is saturated in nitrogen gas. It is then taken to 77K while keeping the sample at approximately 760 Torr. The nitrogen condenses within the pores and can then be measured as the system is slowly brought back to ambient temperatures.

4.3 TEM

TEM stands for Transmission Electron Microscopy. A TEM works like a standard table top microscopy, only instead of passing photons through a thin sample, electrons are used. An image is formed by the transmitted electrons and the focussed on an imaging screen where it is collected either by a photographic film or a CCD camera.

TEMs are useful devices for imaging nano scale material because it has a considerably higher resolution than a traditional microscope. Light microscopes are limited by the wavelength of the light being used and the size of the aperture. Electron Microscopes, on the other hand, utilize the wavelength of the electrons, which can be more finely resolved by changing their kinetic energy according to DeBroglie's equation.

In addition to providing information on electron density, phase, and periodicity, most modern TEMs also are capable of measuring the electron diffraction of a sample.

4.4 Diffraction and Scattering

4.4.1 Electron Diffraction

Electron diffraction describes the crystalline structure of a material. Most electron diffraction is performed with high energy electrons whose wavelengths are orders of magnitude smaller than the inter planar spacings in most crystals. For example, for 100 keV electrons, $\lambda < 3.7 \times 10^{-3}$nm. Typical lattice parameters for crystals are around 0.3 nm.

Transmission electron diffraction is limited because electrons are charged and relatively

light particles. It is therefore necessary for samples to be no thicker than 1 mm to get accurate readings.

4.4.2 IR Absorption

IR absorption tells about what chemicals are bonded to what and helps identify gasses which may be trapped inside the sample. Characteristic peaks indicate bonds between different atoms, making it easy to identify the chemical composition of the material. This is useful in identifying unknown materials but can also verify the presence of non-crystalline structures.

Chapter 5

Experimental Results

5.1 Hydrocarbons Fuels

Only two of the experimental methods attempted resulted in soot production; ultrasonic nebulization and evaporation. Figure (5.1) shows a TEM scan of the soot produced from the ultrasonic method. There is very little soot produced (less than 1 mL) in this method, and it is most likely because the volume fraction of fuel is on the lean side of what is needed.

Unlike the ultrasonic method, the evaporation method did produce soot. Stoichiometric calculations indicate that a detonation in the 100 mL chamber ought to yield 15 mg of sooted carbon. Experimentally we produce approximately 8 mg. The volume of this soot was roughly 2.5 cc which gives a density of approximately 3.2 mg/cc. This is consistant with the findings of Gerving for other liquid drop precursors as well as Dhaubhadel for gasseous precursors[7, 4].

A density of 3.2 mg/cc places this gel on the lower end of the density range of Aerogels. With this basis of comparison, the next test was a BET and a BJH scan. These results are seen in Figures (5.2) and (5.3), respectively. The BET scan indicates a specific surface area

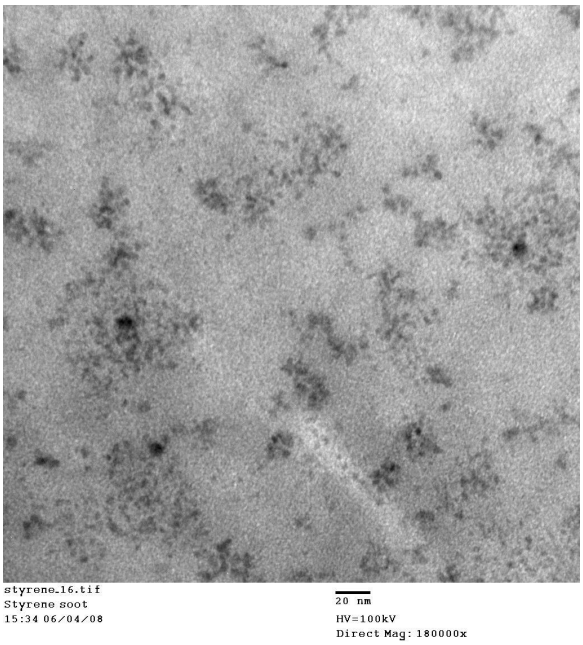

Figure 5.1: Soot produced from a combustion of styrene vapor produced by the Ultra Sonic Nebulizer

of (****) and the BJH shows that the gel has pores.

Aerogels generally have a specific surface area of 400 to 1000 m^2/g and have poresizes around 100 nm. This implies that Aerogels are made of particles which are smaller than Aerosol gels. A TEM confirms this hypothesis. Figure (*Will have figure*) shows that the gel is made of particles approximately (****)nm in diameter. This is smaller compared to gels made by Gerving and Dhaubhadel but larger than the diameters reported for Aerogels and Xerogels.

there will also be a TEM of soot from evaporated Styrene

5.2 Non-Hydrocarbon Fuels

Although the majority of the success of the experiment was with hydrocarbon fuels, there was also a small amount of success with Titanium tetrachloride, $TiCl_4$. This chemical is

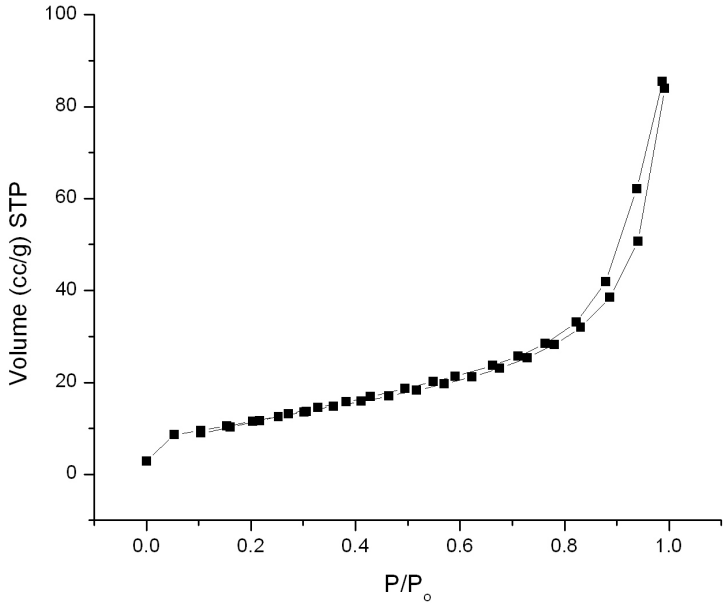

Figure 5.2: A BET scan of styrene soot

extremely hygroscopic and even the best moisture free conditions that we could provide were not enough to prevent a reaction. $TiCl_4$ reacts with water to produce hydrochloric gas and titania particles. Under high temperature or pressure conditions, it can also react with O_2 to make chlorine gas and titania. This is out lined in the reactions below.

$$TiCl_4 + 2H_2O \rightarrow 4HCl + TiO_2 \tag{5.1}$$

$$TiCl_4 + O_2 \rightarrow 4Cl^- + TiO_2 \tag{5.2}$$

$TiCl_4$ also attacks most rubbers and even those which claim to be compatible should be tested as a precaution. This is of particular importance when working within a glovebox, as the chemical will eat through the gloves.

It was difficult to create a moisture free environment to combust the $TiCl_4$. The singular

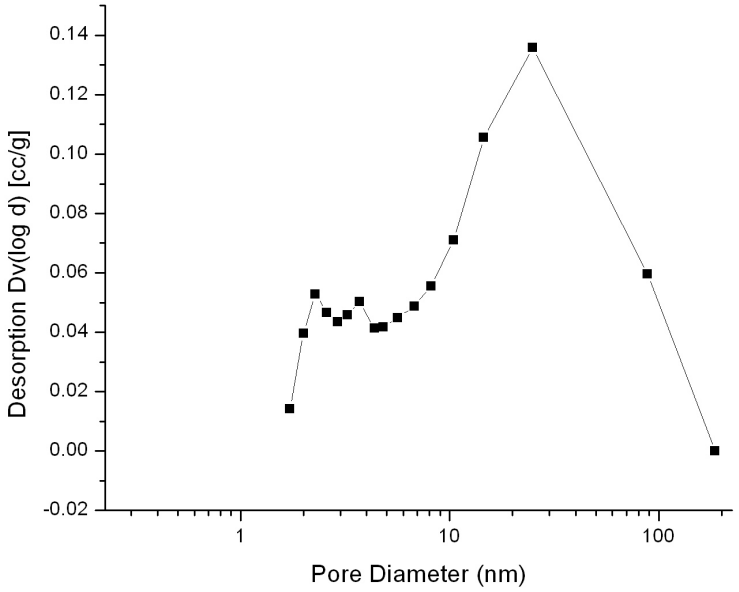

Figure 5.3: A BJH scan of styrene soot

successful trial did not generate a large enough yield for analysis. This was compounded by the problem that $TiCl_4$ does not have as high of a boiling point as do other fuels and therefore was more difficult to ignite.

It was found with the hydrocarbon fuels that the carbon production could be augmented by a carrier combustible gas/O_2 mixture, rather than a carrier gas of pure O_2 . This method successfully augmented the gas phase soot production by 20%. It was logical to attempt to mix $TiCl_4$ with Acetylene gas and this method yielded interesting results.

Aerosol Gels are generally monodispersed in terms of monomer size. The $TiCl_4$ enhanced acetylene combustion, however, produced a bidispersed system, as seen in Figure (5.4). It is believed that the larger particles are titania or Titanium carbide while the smaller particles are Graphitic.

The presence of Titanium carbide was confirmed through an Electron Diffraction scan and the titania was indicated in an IR scan. These results can be seen in Figures (5.5) and

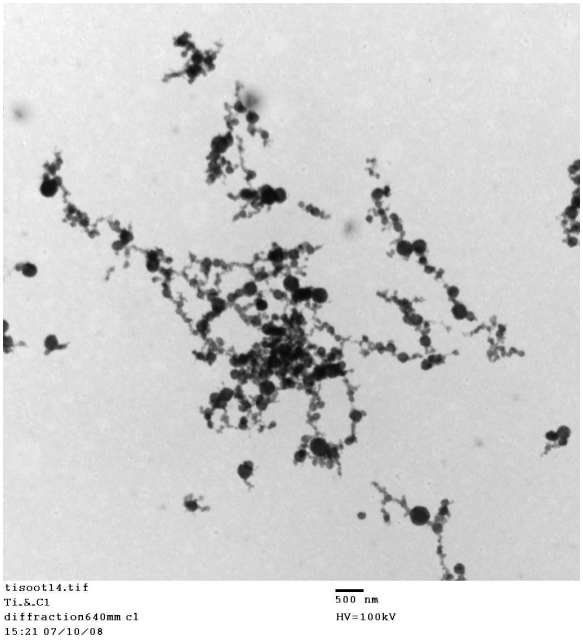

Figure 5.4: A TEM of $TiCl_4$ and Carbon soot

(5.6), respectively.

The gel was further characterized by looking at pore size and surface area. The results of these tests, seen in Figures (5.7) and (5.8), respectively, indicate mostly macropores although it seems to have a similar surface area to other Aerosol Gels. The macropores might be due to the bidispersed nature of the gel which would cause a more irregular packing than a monodispersed system.

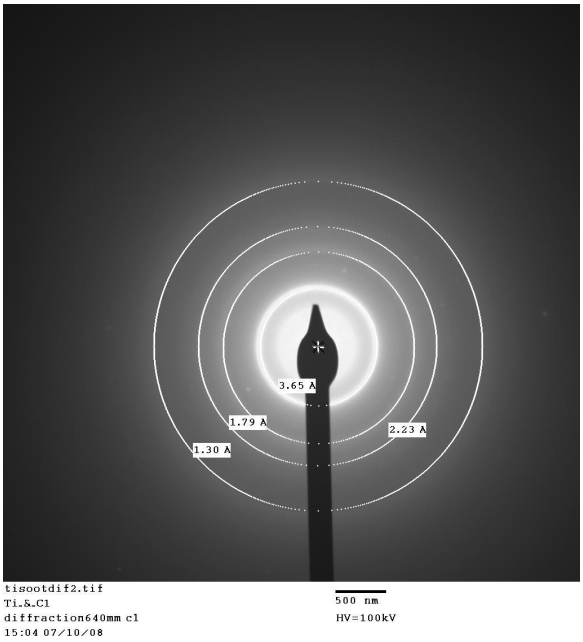

Figure 5.5: Electron diffraction scans of the $TiCl_4$ and Carbon soot

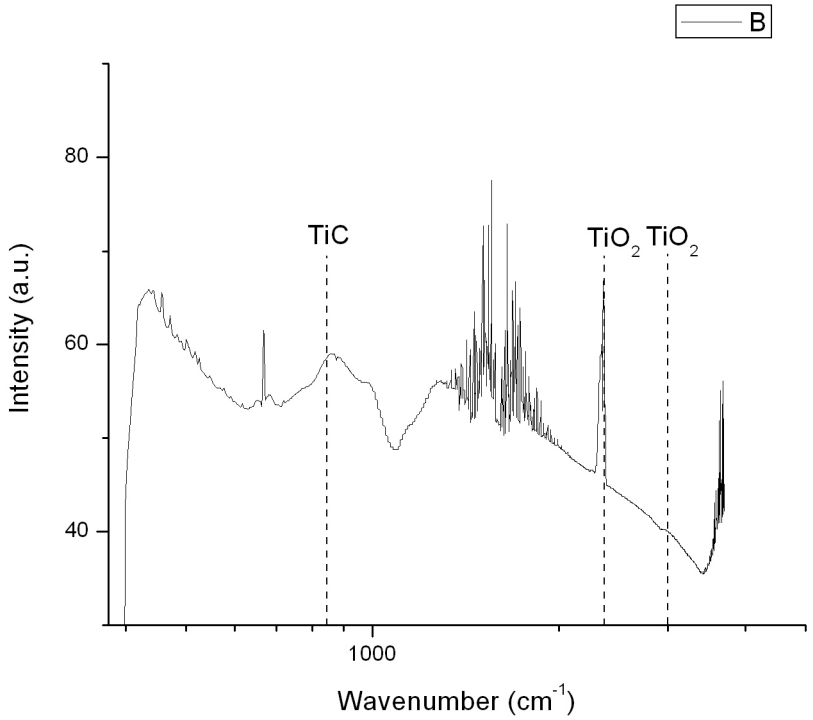

Figure 5.6: Diffraction of IR radiation of the $TiCl_4$ and Carbon soot

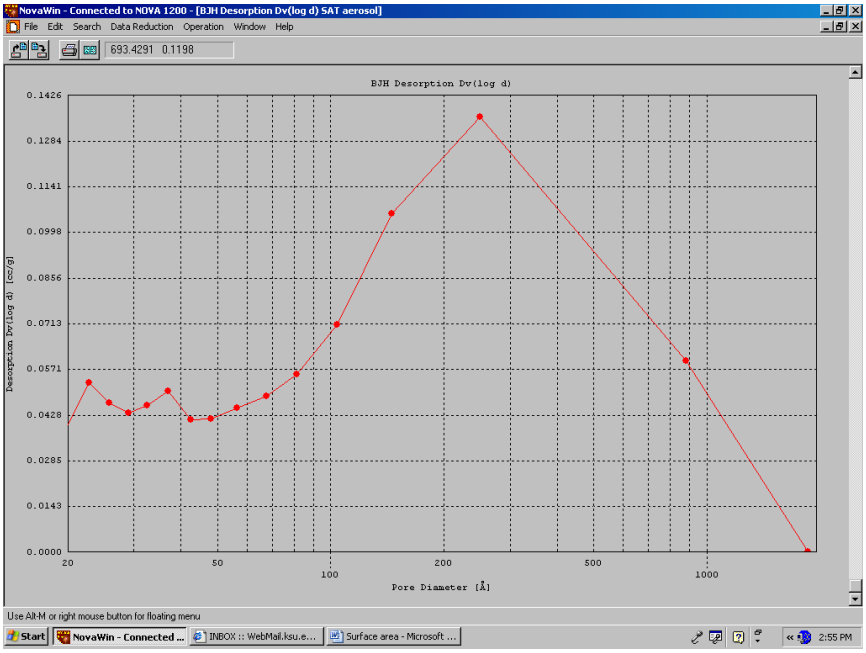

Figure 5.7: Results of the BET Scan indicating pore size of the Ti doped Carbon

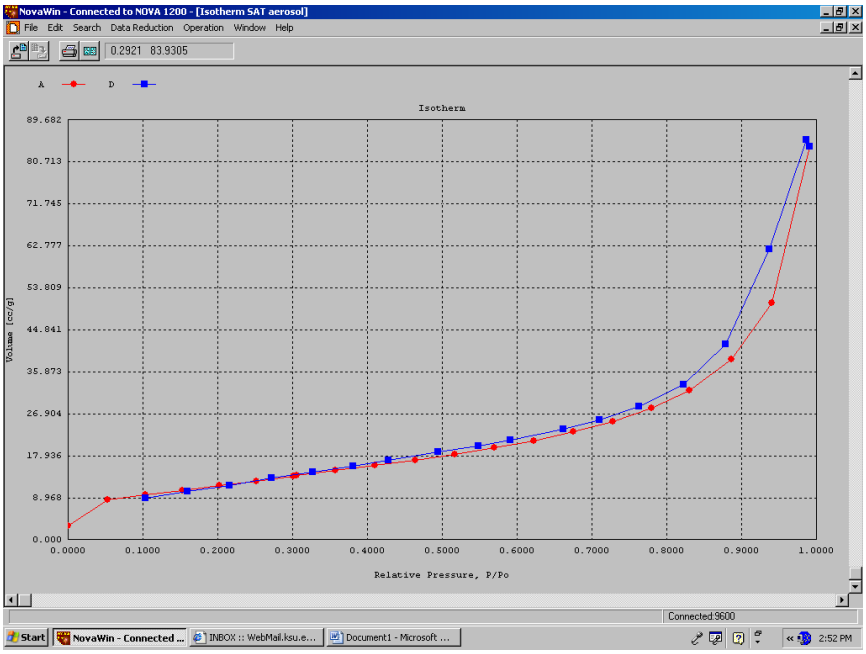

Figure 5.8: Results of the BET Scan indicating surface area of the Ti doped Carbon

Chapter 6

Conclusions

6.1 Discussion of Results

Aerosol Gelation is possible with liquid phase precursors so long as a few conditions are met:

1. *The liquid must be as finely divided as possible.* This increases the surface area and subsequently the amount of fuel exposed to the oxidizing agent. If this condition is not met, the fuel will either not combust or undergoe an incomplete combustion, or burning of the large droplets.

2. *The energy of the spark must be large enough to cause a sustainable combustion.* If insufficient energy is provided to initiate the combustion, the fuel will not fully combust.

3. *The fuel must have a Lower Explosive Limit above the necessary concentration to meet a volume fraction of* 10^{-4}*.* If the concentration is too low, the liquid will not combust. If it does not meet the proper volume fraction condition, the particles will not gel.

4. *The fuel must have a relatively low boiling point.* Without this, it will not combust.

Most of the liquids used in this experiment were hydrocarbons, but a few non-hydrocarbon liquids also meet these requirements.

6.2 Future Work

The purpose of this experiment was to find an effective method for combusting liquid precursors for Aerosol Gelation. That goal was met through the evaporation method. However, the point of using liquid precursors was to expand on potential applications of this form of a gel; one of which being for photocatalytic materials. This is why $TiCl_4$ was used and it is in this context that this I will present directions for future work.

6.2.1 Other Liquids

I feel that further experimentation with $TiCl_4$ is warranted. Extra care must be taken when working with this chemical because of how hygroscopic it is. Still, the prospect of making an Aerosol Gel of Titanium carbide is an exciting one and would most certainly be a novel material worthy of independent study.

Other liquids which are equal troublesome to work with would be Li(***) and Be(****); both of which produce make photocatalytic products when reacted with (****).

6.2.2 Solid Precursors

Aerosol Gelation may also be possible with solid precursors. Metal powders show particular promise because of their readiness to oxidize. Furthermore, metals such as Tungsten, are photocatalytic in their oxidized form. Tungstate, WO_3, is difficult to make using the sol-gel method because few liquid precursors are available. In the context of photocatalytic materials, tungstate may be more desirable than titania as it's band gap is 2.8 eV, rather than 3.7 eV, making it photo-active within the visible spectrum.

For many decades, scientists in Grain Science have been studying the conditions for exploding solids. There is a wealth of literature available, detailing various solids and combustion techniques which have been studied. Popular metals have been Magnesium and Aluminum. The two most popular chamber styles are the Hartmann vertical tube design and the 20 L spherical bomb, both of which have been donated to Dr. Sorensen's lab.

The scientists studying these solid phase combustions were not doing so with the intention of making an Aerosol Gel and it is entirely possible that they have been doing so for many years. Preliminary work carried out by Derek Vermuluen in the summer of 2008 suggests that it is possible to create an aerosol gel from a solid precursor. This is a highly recommended next course of action.

Bibliography

[1] Satcher, J. Available online at https://www.llnl.gov (accessed on Sept 30, 2008), (2005).

[2] Orlando, E. LBNL, http://www.jlab.org/~lyzhu, July (2007).

[3] Longhurst, C. J. http://www.carbibles.com/fuel_engine_bible.html, September (2008).

[4] Gerving, C. S. Master's thesis, Kansas State University, (2004).

[5] Bakrania, S. http://www.vu.union.edu/~bakranis/aerogels/index.htm, March (2003).

[6] Winter, F., editor. *Mathematical modeling and Simulation of Solid Fuel Conversion in Fluidized Bed Combustors: Current Status and Future Developments*. Institute of Chemical Engineering, Vienna University of Technology, (2008).

[7] Dhaudbhadel, R., Gerving, C. S., Chakrabarti, A., and Sorensen, C. M. *Aerosol Science and Technology* **41**, 804–810 (2007).

[8] Finlay, W. H., editor. *The Mechanics of Inhaled Pharmaceutical Aerosols: An Introduction*. Academic Press, (2001).

[9] Tsai, S. C., Chou, Y. F., Cheng, J. H., Song, Y. L., Wang, N., and Tsai, C. S. *IEEE Ultrasonics Symposium* , 1164–1166 (2005).

[10] Brunauer, S., Emmett, P. H., and Teller, E. *J. Am. Chem. Soc.* **60**(2), 309 – 319 (1938).

[11] Roque-Malherbe, R. M. A. *Adsorption and Diffusion in Nanoporous Materials*. CRC Press, (2007).

Appendix A

Critical Time Derivation

We first begin with the Smoluchowski equation

$$\frac{dn}{dt} = -Kn^2$$

By separating the variables and integrating both sides, we should arrive at

$$\frac{1}{Kn} = t_c$$

However, we know that $n = \frac{f_V}{V_{part}}$ so the critical time should be

$$t_c = \frac{V_{part}}{Kf_V} = \frac{4\pi r^3}{3Kf_V}$$

Now, since $K = \frac{8k_BT}{3\eta}$ then

$$t_c = \frac{4\pi r^3 3\eta}{3k_BT8f_V} = \frac{\pi r^3 \eta}{2k_BTf_V} \tag{A.1}$$

Appendix B

Volume Fraction Derivation

From the Extinction Paradox we know that for dense systems, the cross-sectional area from scattering is

$$\sigma \simeq 2\pi r^2$$

where r is the radius of the droplet

Next we must consider the physical situation below, where we have a system of N 3-Dimensional particles being imaged on a plane of area A. This is seen in Figure (B.1)

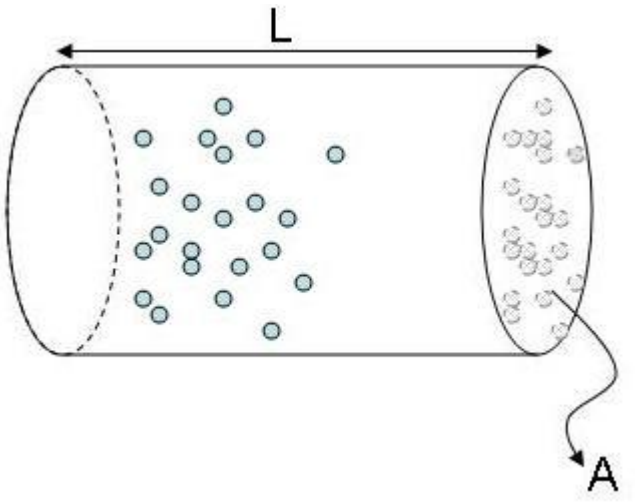

Figure B.1: The blue circles represent 3-dimensional particles and the grey circles represent the imaged particles on a plane A

The relationship between the probability of scattering from a particle is given in Equation (B.1).

$$\langle s \rangle = \frac{N\sigma}{A} \tag{B.1}$$

This is useful, but it is difficult for us to know the exact number of particles in this system so we can make an easy substitution to get:

$$\begin{aligned} \langle s \rangle &= \tfrac{N}{AL}\sigma L \\ &= n\sigma L \end{aligned} \tag{B.2}$$

Where n is the number density of droplets in the Aerosol. At this point it is useful to define the turbidity of the aerosol.

$$\tau = n\sigma \tag{B.3}$$

If we substitute Equation (B.3) into Equation (B.2), we arrive at

$$\langle s \rangle = \tau L \tag{B.4}$$

But we are interested in the probability that light will pass through without striking a single particle. This should indicate the degree of turbidity. For a realistic system, we approximate N to be very large. This means that we have a large possibility of scattering as the light passes through the chamber, but we limit the actual scatter to approximately zero.

$$P(k) = \frac{s^k \exp[-s]}{k!}$$
$$P(0) = \exp[-s]$$

where k is the actual number of scattering events and s is the probability of scattering. By using Equation (B.4) this relation becomes

$$P(0) = \exp[-\tau L] \tag{B.5}$$

Therefore, the probability of zero scattering is dependent only on the turbidity of the aerosol and the length of the light path.

The volume fraction is expressed as

$$f_V = nV_p \tag{B.6}$$

Where V_p is the volume of the particle.

The turbidity is related to the volume fraction by Equation (B.3).

$$f_V = \frac{2}{3} r\tau \tag{B.7}$$

B.1 Turbidity Measurments (Semi-Quantitative)

In order to measure the turbidity of the aerosol, I placed a ruled piece of paper inside of the chamber and then filled the chamber with an aerosol of water. I noted how far I could see into the chamber based off of the rules. This provides a semi-quantitative measurement of

the turbidity, if we assume that

$$I = I_o \exp\left[-\tau L\right]$$

or

$$\tau = \frac{\ln\left[\frac{I}{I_o}\right]}{-L} \tag{B.8}$$

The rules on my paper were spaced 0.385 inches (0.99 cm) and I could only see one rule deep. The total length of the chamber is 4 cm. This means my intensity was attenuated by 0.24. This produces a τ of 0.35 cm^{-1}.

$$f_V = \frac{2}{3}\left(3.4 \times 10^{-4}\right)(0.352) = \boxed{1.2 \times 10^{-4}}$$

Which is in the right limit for aerogel production.

B.2 Measurements of Droplet size via Light Scattering

We placed the sample in a laser beam and measured the intensity of the light passing through the aerosol and then compared it to a calibration measurement. We averaged five points about each of the peaks of these two gaussians to get an average peak intensity for each measurement. By taking the ratio of this average we are able to get the intensity ratio needed in Equation (B.8). This ratio is 0.07, which yeilds a τ of 0.67 cm^{-1}. Thus, the volume fraction is

$$f_V = \frac{2}{3}\left(3.4 \times 10^{-4}\right)(0.314) = \boxed{1.5 \times 10^{-4}}$$

Which is in the correct limit for aerogel production.

Appendix C

Chemical Reactions

C.1 Basic Reactions

The following equations list the stoichiometric equations that dictated the reactant proportions in the experiment.

$$2C_2H_2 + O_2 \rightarrow 2H_2O + 4C \tag{C.1}$$

$$C_7H_8 + 2O_2 \rightarrow 4H_2O + 7C \tag{C.2}$$

$$C_8H_8 + 2O_2 \rightarrow 4H_2O + 8C \tag{C.3}$$

$$TiCl_4 + 2H_2O \rightarrow TiO_2 + 4HCl \tag{C.4}$$

$$TiCl_4 + 2O_2 \rightarrow TiO_2 + 2Cl_2 \tag{C.5}$$

C.2 Styrene Enhanced Combustion

First, let us look to the stochiometric equation for an acetylene combustion.

$$2C_2H_2 \ + O_2 \ \rightarrow \ 2H_2O \ \ + 4C$$

Now let us look at the case of adding a combustible liquid drop vapor. First we will need to estimate the number of moles to include in our stochiometry. The nebulizer generates a volume fraction of 1.8×10^{-4} in a 100 mL chamber. This can be used in the volume fraction relation to determine the total volume of liquid in the chamber:

$$f_V = \frac{NV_p}{V_c}$$

Where V_p and V_c are the volume of the particle and the volume of the chamber respectively. If we define the total volume of liquid as being the number of particles times the volume of each particle, then we can compute the total number of moles of liquid in the chamber.

$$n = \frac{\rho f_V V_c}{\mathcal{M}} \tag{C.6}$$

Entering the appropriate values of styrene into this relation gives $n = 8.7 \times 10^{-5}$mol. The is of course a molecular stochiometric value and not an emprical one, so we must next determine the molecular coefficiants of the other reactants.

We know from the standard Acetylene combustion that 2 moles of C_2H_2 react with 1 mole of O_2 to produce water and carbon. Using the molar gas constant as well as the known volume of the chamber, we can easily determine the number of moles of each reactant.

$$n = \frac{V_c}{22400\text{cc/mol}} = \frac{10^2}{2.24 \times 10^4}\text{mol} = 4.46 \times 10^{-3}\text{mol}$$

Since the O_2 occupies 1/3 of the total volume, 1.48×10^{-3} is equivalent to 1 empirical mole. This tells us that the total number of liquid drop moles in the chamber is

$$n_t = \frac{n_{mol}}{n_{emp}} \tag{C.7}$$

$$n_t = \frac{8.7 \times 10^{-5}}{1.48 \times 10^{-3}} = 5.8 \times 10^{-2} \approx 0.05 = \frac{1}{20}\text{mol}$$

By adding this to the acetylene combustion we get an empirical stochiometric formula of

$$C_8H_8 \ + 40C_2H_2 \ + 22O_2 \ \rightarrow \ 44H_2O \ \ + 88C$$

If we scale this down, it will be easier to compare it to the standard acetylene combustion. Therefore we arrive at:

$$\tfrac{1}{20}C_8H_8 \ + 2C_2H_2 \ + 1.1O_2 \ \rightarrow \ 2.2H_2O \ \ + 4.4C$$

Compared to

$$2C_2H_2 \ + O_2 \ \rightarrow \ 2H_2O \ \ + 4C$$

We see a 10% increase in carbon production from the standard acetylene combustion.

C.3 $TiCl_4$ enhanced combustion

Starting with Equation (1), we must first calculate the number of moles of $TiCl_4$ in the chamber. Substituting the appropriate terms gives a value of $n = 1.15 \times 10^{-4}$mols.

Next, using Equation (2) we can determine the emprical number of moles to be $n = 2.5 \times 10^{-2} \approx \frac{1}{40}$mols.

The next step is to figure out the stoichiometric equation for a $TiCl_4$ enhanced acetylene combustion, but this is somewhat tricky. The reason for this is because the hydrogen atoms from the C_2H_2 could configure in many different ways to form a variety of products. Unlike the styrene enhanced combustion where only carbon and oxygen could accept hydrogen atoms, the $TiCl_4$ enhanced combustion also contributes chlorine.

So, what we need to ask ourselves is where the hydrogens are most likely to go. First let us examine the relative electronegativities of all of the elements involved. Using the Pauling scale, the table below shows the relative electronegativity of each of these elements.

Table C.1: The relative electronegativities of the elements involved in the $TiCl_4$ enhanced acetylene combustion.

Element	Relative Electronegativity
Ti	1.5
H	2.2
C	2.5
Cl	3.1
O	3.4

A polar bond can be defined as one between an atom with high electronegativity and an atom with low electronegativity. The more polar a molecule, the easier it is to break the bonds and the easier it is to make them again. It is reasonable to assume that given a choice, the atom is more likely to enter into a polar bond than a non-polar bond.

With this in consideration, we can see that the most likely stoichiometric configuration for the $TiCl_4$ enhanced acetylene combustion is

$$TiCl_4 + 80\ C_2H_2 + 40O_2 \rightarrow TiO_2 + 4\ HCl + 78H_2O + 160\ C$$

If we scale this down we can compare it to the other reactions.

$$\tfrac{1}{40}TiCl_4 + 2C_2H_2 + O_2 \rightarrow \tfrac{1}{40}TiO_2 + \tfrac{1}{10}\ HCl + 1.95H_2O + 4\ C$$